Penerbit Akademia Baru

Journal of Advanced Research in Applied Mechanics

Journal homepage: www.akademiabaru.com/aram.html
ISSN: 2289-7895

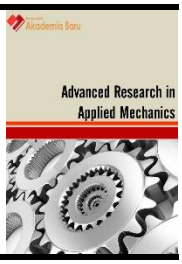

Heat Transfer Enhancement in Straight Channel with Nanofluid In Fully Developed Turbulent Flow

Open Access

Abdolbaqi Mohammed Khdher[1], Nor Azwadi Che Sidik[1,*], Siti Nurul Akmal Yusof[1], M'hamed Beriache[2]

[1] Malaysia – Japan International Institute of Technology (MJIIT), University Teknologi Malaysia, Jalan Sultan Yahya Petra,54100 Kuala Lumpur, Malaysia
[2] Department of Mechanical Engineering, Faculty of Technology, University Hassiba Benbouali, Algeria

ABSTRACT

A numerical study for investigating the secondary flow configuration in square straight channel with hydraulic diameter of 0.02m and heat transfer enhancement of water and three different types of nanofluids (Al2O3, TiO2 and CuO) in water as base fluid under constant heat flux in upper and lower walls. The study conducted at steady state, turbulent forced convection and three-dimensional flows. Certain boundary conditions and assumptions to solve the governing equations were implemented with using finite volume method. CFD software's involving GAMBIT and FLUENT were employed to perform the investigation numerically in the range of Reynolds number 104-106. The results show that by increasing Reynolds number the secondary flow increase as well as shear stress is increased, the boundary layers decrease and increase the gradient velocity near a wall. As the volume concentration increases, the wall shear stress and heat transfer rates increase. The three types of nanofluids achieved higher Nusselt number while the friction factor of all of them was seen at similar values. Nanofluid with CuO, nanoparticle achieved the highest Nusselt number followed by TiO2 and Al2O3, respectively while the pure water came last in considered range of Reynolds number. The Nusselt number CuO-water increased with the increase of volume fraction and with the increase of Reynolds number. Reynolds number caused to enhance Nusselt number for all cases. The local Nusselt number for CuO-water increased with increase of Reynolds number.

Keywords:
secondary flow; nanofluids; Reynolds number

1. Introduction

Heat transfer knowledge has been considered since long times ago. High efficiency of heat transfer has improved not only performance of the devices, but also fuel consumption. The efficiency of many devices which are needed to be heated or cooled is involved to heat transfer performance. The necessity of high thermal performance thermal systems has been eventuated finding different ways to enhance heat transfer rate.

Straight channels are widely used in electronic devices, heat exchangers, cooling of gas turbine blade, gas-cooled nuclear reactors and solar air heater ducts, etc. The heat transfer enhancement in a channels and pipes according to many factors, walls materials, fluids flow types inside them, fluid thermal properties, etc. The enhancement of heat transfer generally means the increase in heat

* *Corresponding author.*
E-mail address: azwadi@utm.my (Nor Azwadi Che Sidik)

transfer rate, from Newton's law of cooling, and the overall heat transfer equations it can be observe that by increasing in (convection heat transfer coefficient, thermal conductivity, surface area and deference between the surface and fluid temperature) the heat transfer rate can be increased. The enhancement techniques mean the methods or ways by which the value of thermal conductivity (k) or convection heat transfer coefficient (h) can be increased. There are many methods of heat transfer enhancement, the principles of these methods are decreasing the thermal boundary layer thickness, increasing the interruption in fluids and increasing the velocity gradient near a wall.

The secondary flow in the straight channels and ducts generated by the turbulent Reynolds stresses, as well as by the pressure gradient normal to the stream wise flow, which link the small-scale turbulent fluctuations to the large-scale secondary flow. The effect of the secondary flow is to transport slow-moving fluid away from the wall at the channel center, while moving fast-moving fluid from the channel core towards the corner to increasing the wall stress there, this lead to decreasing the boundary layer and enhance the heat transfer by increasing Nusselt's number. This type of secondary flow known as "stress-induced secondary flows" and is due to the anisotropy of the normal Reynolds stresses [1-2].

In general, secondary flows can be classified into two types, namely, Prandtl's secondary flows of the first and second kind. The former involves secondary flows via centrifugal force in a curved channel, while the latter involves secondary flows due to the anisotropy of turbulence in a straight open channel or duct. Secondary flows are important in engineering practice because they affect the mean flow and turbulent structures. As a result, many experimental and numerical studies have been performed in attempts to understand the underlying physics of secondary flows [3-7]. Thangam and Speziale [5] studied secondary flow that occurs in the transverse planes of the duct which causes fluid particles to undergo a spiralling motion down the duct in contrast to the rectilinear particle paths in a Newtonian fluid as shown in Figure 1.

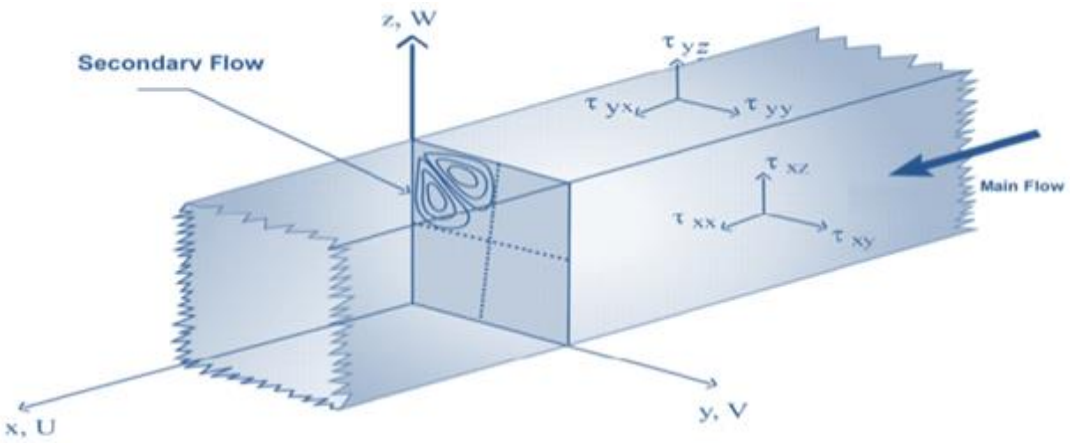

Fig. 1. Secondary flow in a square duct

However, there is a limitation of the secondary flow, which is that the effect of the secondary flow is to transport the fluid moving slowly from the wall in the center of the channel, while moving the fluid moving rapidly from the channel core to the corner, increasing the pressure wall there and results to the decreasing the boundary layer and heat transfer rate. Thus, to overcome this limitation, many researchers has focusses to enhance the heat transfer rate of the secondary flow in straight channel [8-11]. One of the most effective method is to use nanofluid. Nanofluids are engineered

colloids made of a base fluid and nanoparticles. Nanoparticles are particles that are between 1 and 100 nm in diameter. Nanofluids typically employ metal or metal oxide nanoparticles, such as copper and alumina, and the base fluid is usually a conductive fluid, such as water or ethylene glycol [12-13].

Nanofluids are studied because of their heat transfer properties: they enhance the thermal conductivity and convective properties over the properties of the base fluid [14]. Enhancement of convective heat transfer and thermal conductivity of liquids was earlier made possible by mixing micron sized particles with a base fluid [15]. However, rapid sedimentation, erosion, clogging and high-pressure drop caused by these particles has kept the technology far from practical use. A very small number of nanoparticles was dispersed uniformly and suspended stably in base fluids, it can provide impressive improvements in the thermal properties of base fluids.

The heat transfer resistance of a flowing fluid is most often represented by a Nusselt number, which considers the fluid thermal conductivity. Thus, the primary assessment of the heat transfer potential of nanofluids is to consider its thermal conductivity. The physical mechanism accounting for the thermal conductivity of nanofluids is not well understood. Maxwell was one of the first investigators of suspended panicles. He considered a very dilute suspension of spherical particles by ignoring the interactions among the particles and made an equation that can be applied for particles with low volume concentrations. A great number of extensions to the Maxwell equation have been carried out since Maxwell's initial investigation. These extensions consider various factors related to effective thermal conductivity, including particle shape [16] particle distribution, high volume concentration, particle-shell structure, and contact resistance. In addition, the thermal conductivity enhancement ratio is defined as the ratio of the thermal conductivity of the nanofluids to the thermal conductivity of the base fluid. This enhancement can be affected by different parameters. Such as particle volume concentration, particle material, particle size, particle shape, base fluid material, temperature, additive, and acidity. Many study and research have been proposed to measure and explain the thermal conductivity of nanofluids [17-21].

The effects of several important factors such as particle size on the effective thermal conductivity of nanofluids have not been studied adequately. It is important to do more research to ascertain the effects of these factors on the thermal conductivity of wide range of nanofluids. The size of nanoparticles is in the range of 1-100 nm for nanofluids. The smaller in particle size higher will be the enhancement. Since the surface to volume ratio will be higher for small diameter particles which results in uniform distribution of particles gives and the best enhancement. On the other hand, even when the particle size of CuO was smaller than that of Al_2O_3 the deterioration in heat transfer was greater with Al_2O_3. This is because the particle density of CuO is higher than Al_2O_3 [22]. Compared to micron-sized particles, nanoparticles are engineered to have larger relative surface areas, less 203 particle momentum, high mobility and better suspension stability than micron-sized particles and importantly increase the thermal conductivity of the mixture.

In addition, it is reported that as the size of nanoparticle reduce, the Brownian motion will be induced [23]. The most used geo metric shape of the particles is spherical and cylindrical. The cylindrical particles show an increase in thermal conductivity enhancement due to a mesh formed by the elongated particles that conducts heat through the fluid. This indicates the elongated particles are superior to spherical for thermal conductivity [24]. The size of nanoparticles in the host liquid is too important to the new and compact technology. It can be used in small size system such as nano systems and micro-passages where the clog is avoided. According to Rostamani *et al.,* [25] the turbulent flow of nanofluids with different volume concentrations of nanoparticles flowing through a two-dimensional duct under constant heat flux condition is analysed numerically. The nanofluids considered are mixtures of CuO, Al_2O_3 and TiO_2 nanoparticles and water as the base fluid. All the thermophysical properties of nanofluids are temperature dependent. The viscosity of nanofluids is

obtained on basis of experimental data. However, study on the configuration of secondary flow and convection heat transfer phenomenon in a fully developed turbulent flow inside a long horizontal duct of CuO, Al_2O_3 and TiO_2 nanoparticles has been minimally reported.

The purpose of this study is to investigate the configuration of secondary flow and convection heat transfer phenomenon and pressure drop of three different nanofluids in a fully developed turbulent flow inside a long horizontal duct. The standard k-ε model is used to predict the kinetic energy and its dissipation rate in the turbulent flow. Here, the nanofluid is the mixture of water as the base fluid and CuO, Al2O3 and TiO2 nanoparticles with different volume concentration. All the thermophysical properties of nanofluids are temperature dependent. The Reynolds number at the inlet section varied from 10,000 to 1000,000.

2. Methodology

2.1 Description of the Problem and Conservation Equations

The nanoparticles in the base fluid may be easily fluidized and consequently the effective mixture behaves like a single-phase fluid [21]. It is also assumed that the fluid phase and nanoparticles are in thermal equilibrium with zero relative velocity. This may be realistic as nanoparticles are much smaller than micro particles and the relative velocity decreases as the particle size decreases. The resultant mixture may be considered as a conventional single-phase fluid. Under these assumptions, the classical theory of single-phase fluid can be applied to nanofluids. The channel material is homogeneous and isotropic. The thermal conductivity of the channel wall material does not change with temperature and the flow is steady, fully developed, turbulent, and three –dimensional. The governing equations to be considered are the time-averaged incompressible continuity, momentum and energy equations.

It is generally accepted that the Navier-Stokes momentum equations are valid for turbulent flow if the parameters are considered to consist of a mean and fluctuating component $(\text{e.g. } u = \bar{u} + \acute{u})$.

The Reynold's Number obtained by a substitution of mean and fluctuating into the incompressible Naver-Stokes equations, and taking time averages are:

$$\frac{\partial \bar{u}}{\partial t} + \bar{u}\frac{\partial \bar{u}}{\partial x} + \bar{v}\frac{\partial \bar{u}}{\partial y} + \bar{w}\frac{\partial \bar{u}}{\partial z} = -\frac{1}{\rho}\frac{\partial \bar{p}}{\partial x} + \nu \boldsymbol{\nabla^2}\bar{u} - \left[\frac{\partial}{\partial x}\left(\overline{\acute{u}^2}\right) + \frac{\partial}{\partial y}\left(\overline{\acute{u}\acute{v}}\right) + \frac{\partial}{\partial z}\left(\overline{\acute{u}\acute{w}}\right)\right]$$

$$\frac{\partial \bar{v}}{\partial t} + \bar{u}\frac{\partial \bar{v}}{\partial x} + \bar{v}\frac{\partial \bar{v}}{\partial y} + \bar{w}\frac{\partial \bar{v}}{\partial z} = -\frac{1}{\rho}\frac{\partial \bar{p}}{\partial y} + \nu \boldsymbol{\nabla^2}\bar{v} - \left[\frac{\partial}{\partial x}\left(\overline{\acute{u}\acute{v}}\right) + \frac{\partial}{\partial y}\left(\overline{\acute{v}^2}\right) + \frac{\partial}{\partial z}\left(\overline{\acute{v}\acute{w}}\right)\right]$$

$$\frac{\partial \bar{w}}{\partial t} + \bar{u}\frac{\partial \bar{w}}{\partial x} + \bar{v}\frac{\partial \bar{w}}{\partial y} + \bar{w}\frac{\partial \bar{w}}{\partial z} = -\frac{1}{\rho}\frac{\partial \bar{p}}{\partial z} + \nu \boldsymbol{\nabla^2}\bar{w} - \left[\frac{\partial}{\partial x}\left(\overline{\acute{u}\acute{w}}\right) + \frac{\partial}{\partial y}\left(\overline{\acute{v}\acute{w}}\right) + \frac{\partial}{\partial z}\left(\overline{\acute{w}^2}\right)\right] \quad (1)$$

The equation of continuity for steady incompressible flow may be written as

$$\frac{\partial \bar{u}}{\partial x} + \frac{\partial \bar{v}}{\partial y} + \frac{\partial \bar{w}}{\partial z} = 0 \quad (2)$$

A continuity equation also may be written for the instantaneous fluctuating equations as

$$\frac{\partial \acute{u}}{\partial x} + \frac{\partial \acute{v}}{\partial y} + \frac{\partial \acute{w}}{\partial z} = 0 \quad (3)$$

The problem under consideration here is that of a fully developed steady channel flow (mean values do not very with time or x). Therefore, all the derivatives with respect to time and axial distance (x) vanish yielding the following set of equations for fully developed steady flow.

$$\frac{\partial \bar{v}}{\partial y}+\frac{\partial \bar{w}}{\partial z}=0 \tag{4}$$

$$\bar{v}\frac{\partial \bar{u}}{\partial y}+\bar{w}\frac{\partial \bar{u}}{\partial z}=-\frac{1}{\rho}\frac{\partial \bar{p}}{\partial x}+\nu\boldsymbol{\nabla^2}\bar{u}-\frac{\partial}{\partial y}\left(\overline{\acute{u}\acute{v}}\right)-\frac{\partial}{\partial z}\left(\overline{\acute{u}\acute{w}}\right)$$

$$\bar{v}\frac{\partial \bar{v}}{\partial y}+\bar{w}\frac{\partial \bar{v}}{\partial z}=-\frac{1}{\rho}\frac{\partial \bar{p}}{\partial y}+\nu\boldsymbol{\nabla^2}\bar{v}-\frac{\partial}{\partial y}\left(\bar{\acute{v}}^2\right)-\frac{\partial}{\partial z}\left(\overline{\acute{v}\acute{w}}\right)$$

$$\bar{v}\frac{\partial \bar{w}}{\partial y}+\bar{w}\frac{\partial \bar{w}}{\partial z}=-\frac{1}{\rho}\frac{\partial \bar{p}}{\partial z}+\nu\boldsymbol{\nabla^2}\bar{w}-\frac{\partial}{\partial y}\left(\overline{\acute{v}\acute{w}}\right)+\frac{\partial}{\partial z}\left(\bar{\acute{w}}^2\right) \tag{5}$$

It is enlightening to consider the equations of motion in slightly different form. By combining successive pairs of the Reynold's momentum Eq. (1) in a manner to eliminate the pressure terms and then simplifying using the continuity relation in Eq. (2), the vorticity equations with Reynold's stresses are obtained (after considerable manipulation).

$$\frac{\partial \bar{\xi}}{\partial t}+\bar{u}\frac{\partial \bar{\xi}}{\partial x}+\bar{v}\frac{\partial \bar{\xi}}{\partial y}+\bar{w}\frac{\partial \bar{\xi}}{\partial z}=\bar{\xi}\frac{\partial \bar{u}}{\partial x}+\bar{\eta}\frac{\partial \bar{u}}{\partial y}+\bar{\zeta}\frac{\partial \bar{u}}{\partial z}+\nu\boldsymbol{\nabla^2}\bar{\xi}+\frac{\partial^2}{\partial x\partial z}\left(\overline{\acute{u}\acute{v}}\right)+\frac{\partial^2}{\partial y\partial z}\left(\bar{\acute{v}}^2\right)+\frac{\partial^2}{\partial z^2}\left(\overline{\acute{v}\acute{w}}\right)-\frac{\partial^2}{\partial x\partial y}\left(\overline{\acute{u}\acute{w}}\right)-\frac{\partial^2}{\partial y^2}\left(\overline{\acute{v}\acute{w}}\right)-\frac{\partial^2}{\partial y\partial z}\left(\bar{\acute{w}}^2\right)$$

$$\frac{\partial \bar{\eta}}{\partial t}+\bar{u}\frac{\partial \bar{\eta}}{\partial x}+\bar{v}\frac{\partial \bar{\eta}}{\partial y}+\bar{w}\frac{\partial \bar{\eta}}{\partial z}=\bar{\xi}\frac{\partial \bar{v}}{\partial x}+\bar{\eta}\frac{\partial \bar{v}}{\partial y}+\bar{\zeta}\frac{\partial \bar{v}}{\partial z}+\nu\boldsymbol{\nabla^2}\bar{\eta}+\frac{\partial^2}{\partial x^2}\left(\overline{\acute{u}\acute{w}}\right)+\frac{\partial^2}{\partial x\partial y}\left(\overline{\acute{v}\acute{w}}\right)+\frac{\partial^2}{\partial x\partial z}\left(\bar{\acute{w}}^2\right)-\frac{\partial^2}{\partial x\partial z}\left(\bar{\acute{u}}^2\right)-\frac{\partial^2}{\partial y\partial z}\left(\overline{\acute{u}\acute{v}}\right)-\frac{\partial^2}{\partial z^2}\left(\overline{\acute{u}\acute{w}}\right)$$

$$\frac{\partial \bar{\zeta}}{\partial t}+\bar{u}\frac{\partial \bar{\zeta}}{\partial x}+\bar{v}\frac{\partial \bar{\zeta}}{\partial y}+\bar{w}\frac{\partial \bar{\zeta}}{\partial z}=\bar{\xi}\frac{\partial \bar{w}}{\partial x}+\bar{\eta}\frac{\partial \bar{w}}{\partial y}+\bar{\zeta}\frac{\partial \bar{w}}{\partial z}+\nu\boldsymbol{\nabla^2}\bar{\zeta}+\frac{\partial^2}{\partial x\partial y}\left(\bar{\acute{u}}^2\right)+\frac{\partial^2}{\partial y^2}\left(\overline{\acute{u}\acute{v}}\right)+\frac{\partial^2}{\partial y\partial z}\left(\overline{\acute{u}\acute{w}}\right)-\frac{\partial^2}{\partial x^2}\left(\overline{\acute{u}\acute{v}}\right)-\frac{\partial^2}{\partial x\partial y}\left(\bar{\acute{v}}^2\right)-\frac{\partial^2}{\partial x\partial z}\left(\overline{\acute{v}\acute{w}}\right) \tag{6}$$

where the vorticity components are defined by

$$\xi=\frac{\partial w}{\partial y}-\frac{\partial \bar{v}}{\partial z}\quad;\quad \eta=\frac{\partial u}{\partial z}-\frac{\partial w}{\partial x}\quad;\quad \zeta=\frac{\partial v}{\partial x}-\frac{\partial u}{\partial y} \tag{7}$$

A continuity equation for vorticity takes a form analogous to Eq. (2)

$$\frac{\partial \bar{\xi}}{\partial x}+\frac{\partial \bar{\eta}}{\partial y}+\frac{\partial \bar{\zeta}}{\partial z}=0\quad also\ \frac{\partial \acute{\xi}}{\partial x}+\frac{\partial \acute{\eta}}{\partial y}+\frac{\partial \acute{\zeta}}{\partial z}=0 \tag{8}$$

This is easily demonstrated by substitution of the vorticity definitions into Eq. (8). Considerable simplification of Eq. (6) is attained by the restriction to a steady, fully developed flow. The vorticity equations then reduce to Eqs. (9) to (11)

$$\bar{v}\frac{\partial \bar{\xi}}{\partial y}+\bar{w}\frac{\partial \bar{\xi}}{\partial z}=\nu\boldsymbol{\nabla^2}\bar{\xi}+\frac{\partial^2}{\partial y\partial z}\left(\bar{\acute{v}}^2-\bar{\acute{w}}^2\right)-\frac{\partial^2}{\partial y^2}\left(\overline{\acute{v}\acute{w}}\right)+\frac{\partial^2}{\partial z^2}\left(\overline{\acute{v}\acute{w}}\right) \tag{9}$$

$$\bar{v}\frac{\partial\bar{\eta}}{\partial y}+\bar{w}\frac{\partial\bar{\eta}}{\partial z}=\bar{\eta}\frac{\partial\bar{v}}{\partial y}+\bar{\zeta}\frac{\partial\bar{v}}{\partial z}+\nu\nabla^2\bar{\eta}-\frac{\partial^2}{\partial y\partial z}\left(\overline{\acute{u}\acute{v}}\right)-\frac{\partial^2}{\partial z^2}\left(\overline{\acute{u}\acute{w}}\right) \tag{10}$$

$$\bar{v}\frac{\partial\bar{\zeta}}{\partial y}+\bar{w}\frac{\partial\bar{\zeta}}{\partial z}=\bar{\eta}\frac{\partial\bar{w}}{\partial y}+\bar{\zeta}\frac{\partial\bar{w}}{\partial z}+\nu\nabla^2\bar{\zeta}+\frac{\partial^2}{\partial y^2}\left(\overline{\acute{u}\acute{v}}\right)+\frac{\partial^2}{\partial y\partial z}\left(\overline{\acute{u}\acute{w}}\right) \tag{11}$$

Eqs. (10) and (11) can be shown by appropriate manipulation to be identical. Therefore Eqs. (9) to (11) represents only 2 independent equations. From the axial momentum equation in Eq. (9), the cause of the secondary flows can be seen in broad, general terms. The vorticity component $(\bar{\xi})$ represents a mean rotation of a fluid element about an axial parallel to the channel axis.

The turbulent motion in flow causes significant fluctuation of flow properties (i.e. velocity, pressure, temperature and even density (if compressible flow)). By decomposing the flow properties such as velocity component u into an average value and a fluctuation component, the equation for turbulence fluctuation is obtained

$$u=\bar{u}+u' \tag{12}$$

where $\bar{u}$ is the average velocity and u' is the fluctuating velocity. The average value of independent time for steady turbulent motion is expresses as

$$\bar{f}=\frac{1}{\Delta\tau_1}\int_0^{\Delta r_1} f d\tau \tag{13}$$

The time interval $\Delta\tau$, is taken large enough to exceed amply the period of the fluctuations. On the other hand, the time average of the fluctuations, f' is zero:

$$\bar{f}'=\frac{1}{\Delta\tau_1}\int_0^{\Delta r_1} f' d\tau=\frac{1}{\Delta\tau_1}\int_0^{\Delta r_1}(f-f')d\tau=\bar{f}-\bar{f}=0 \tag{14}$$

where, f may denote any flow parameter.

The governing equations for steady turbulent flows can be expressed as;

$$\frac{\partial\bar{u}}{\partial x}+\frac{\partial\bar{v}}{\partial y}+\frac{\partial\bar{w}}{\partial z}=0 \tag{15}$$

$$\rho\left(\bar{u}\frac{\partial\bar{u}}{\partial x}+\bar{v}\frac{\partial\bar{u}}{\partial y}+\bar{w}\frac{\partial\bar{u}}{\partial z}\right)=-\frac{\partial\bar{\rho}}{\partial x}+\mu\nabla^2\bar{u}-\frac{\partial}{\partial x}\rho\overline{u^{12}}-\frac{\partial}{\partial y}\rho\overline{u'v'}-\frac{\partial}{\partial z}\rho\overline{u'w'} \tag{16}$$

$$\rho\left(\bar{u}\frac{\partial\bar{v}}{\partial x}+\bar{v}\frac{\partial\bar{v}}{\partial y}+\bar{w}\frac{\partial\bar{v}}{\partial z}\right)=-\frac{\partial\bar{\rho}}{\partial y}+\mu\nabla^2\bar{v}-\frac{\partial}{\partial x}\rho\overline{u'v'}-\frac{\partial}{\partial y}\rho\overline{w^{12}}-\frac{\partial}{\partial z}\rho\overline{v'w'} \tag{17}$$

$$\rho\left(\bar{u}\frac{\partial\bar{w}}{\partial x}+\bar{v}\frac{\partial\bar{w}}{\partial y}+\bar{w}\frac{\partial\bar{w}}{\partial z}\right)=-\frac{\partial\bar{\rho}}{\partial z}+\mu\nabla^2\bar{w}-\frac{\partial}{\partial x}\rho\overline{u'w'}-\frac{\partial}{\partial y}\rho\overline{v'w'}-\frac{\partial}{\partial z}\rho\overline{w^{12}} \tag{18}$$

$$\rho c_p\left(\bar{u}\frac{\partial \dot{t}}{\partial x}+\bar{v}\frac{\partial \dot{t}}{\partial y}+\bar{w}\frac{\partial \dot{t}}{\partial z}\right)=k\nabla^2 t-\frac{\partial}{\partial x}\rho c_p\overline{u't'}-\frac{\partial}{\partial y}\rho c_p\overline{v't'}-\frac{\partial}{\partial z}\rho c_p\overline{w't'} \quad (19)$$

where

$$\nabla^2=\frac{\partial^2}{\partial x^2}+\frac{\partial^2}{\partial y^2}+\frac{\partial^2}{\partial z^2} \quad (20)$$

The governing equations of the incoming fluid flow are non-linear and coupled with partial differential equations and it is subjected to the boundary conditions. It is assumed that the incoming flow through the total length is steady forced turbulent at ambient temperature ($T_{in}=293K$), and pressure with uniform velocity ($u_{in}=u_i;\ u_j=0$) and constant heat flux for upper and bottom wall of ($q''=50000\frac{w}{m^2}$), and for lift and right side the temperature is ($T_w=293K^o$) and the flow enters the test section with fully developed profile.

In the present work the $(k-\varepsilon)$ model proposed by Rostamani *et al.,* [25]. Constants and functions value are Cμ=0.009, C1ε=1.44, C2ε=1.92, σ_k=1, σ_ε=1.3 and Pr=0.09. Different fluid velocities enter the geometry and they vary to ensure Reynolds numbers in the range of 10000-1000000. Outflow boundary condition has been implemented for the outlet section. Eqs. (21) to (23) are used to calculate the turbulent intensity (I), turbulent kinetic energy (k) and turbulent dissipation rate (ε) at the inlet section of the duct [26].

$$I=0.16\,\mathrm{Re}^{\frac{-1}{8}} \quad (21)$$

$$K=\frac{3}{2}\left(I\times U_{in}\right)^2 \quad (22)$$

$$\varepsilon=C_\mu^{0.75}\frac{K^{1.5}}{0.1h} \quad (23)$$

The Nusselt numbers, the Reynolds number, the Darcy friction factor, the performance evaluation criteria and pumping power in case of the present study were calculated respectively, as follows:

$$Nu=\frac{\boldsymbol{h}d_h}{k} \quad (24)$$

$$Re=\frac{\rho u_m d_h}{\mu} \quad (25)$$

$$f=\frac{2\Delta P d_h}{L\rho u_m^2} \quad (26)$$

where the ΔP is pressure difference between inlet and outlet:

$$\Delta P=P_{ave,inlet}-P_{ave,outlet} \quad (27)$$

Hence, $P_{ave,inlet}$, $P_{ave,outlet}$ are the inlet and outlet pressures, respectively.

The Darcy friction factor determines the pump or fan power requirements and it can be calculated by using Fanning friction factor as follows [27]:

$$f = 4C_f \tag{28}$$

Fanning friction factor is defined as follows [28]:

$$C_f = \frac{2\tau_w}{\rho u_m^2} \tag{29}$$

where, τ_w is the wall shear stress.

Nusselt numbers correlations are a classical expression for computing the local Nusselt number for fully developed turbulent flow in both hydrodynamically and thermally profile in smooth channels. The Pak and Cho equation [29] is expressed as

$$Nu = 0.021Re^{0..80}Pr^{0.5} \tag{30}$$

This equation has been confirmed experimentally for the range of conditions

i. The Prandtl numbers are in the range of $6.54 \leq Pr \leq 12.33$
ii. The value of Reynolds numbers is $10^4 \leq Re \leq 10^5$

The Gnielinski correlation applies for both uniform surface heat flux and temperature for smooth tubes with fully developed flow condition of the form [30]:

$$Nu = 0.012(Re^{0..87} - 280)Pr^{0.4} \tag{31}$$

It is valid for Prandtl and Reynolds numbers in the ranges of $1.5 \leq Pr \leq 500$ and $3 \times 10^3 \leq Re \leq 10^6$, respectively.

The friction factor is function of Reynolds number and the channel wall condition. It is low for smooth wall and increases with increasing surface roughness. Blasius correlation determined the friction factor of the form [31]:

$$f = 4C_f = 4(0.0791\mathrm{Re}^{\frac{-1}{4}} \tag{32}$$

In order to simulate nanofluids, effective properties of them must be calculated first. In this study nanoparticles being considered areAl_2O_3, CuO, and TiO_2. Required properties for simulation are effective thermal conductivity (k_{eff}), effective dynamic viscosity (μ_{eff}), effective mass density(ρ_{eff}), and the effective specific heat (C_{peff}).

The density of nanofluids can be obtained from following equation [32]:

$$\rho_{nf} = (1 - \phi)\rho_f + \phi\rho_{np} \tag{33}$$

where ρ_f and ρ_{np} are mass densities of base fluid and NPs, respectively.

Heat Capacity is calculated using following equation:

$$(\rho C_p)_{nf} = (1-\phi)(\rho C_p)_f + \phi(\rho C_p)_{np} \quad (34)$$

where $(\rho C_p)_f$ and $(\rho C_p)_{np}$ are heat capacities of base fluid and NPs, respectively.

Considering the Brownian motion, effective thermal conductivity of nanofluid can be obtained using following mean empirical correlation:

$$k_{eff} = k_{static} + k_{Brownian} \quad (35)$$

$$k_{static} = k_f \left[\frac{(k_{np}+2k_f)-2\phi(k_f-k_{np})}{(k_{np}+2k_f)+\phi(k_f-k_{np})}\right] \quad (36)$$

$$k_{brownian} = 5\times 10^4 \beta\phi\rho_f C_{p,f}\sqrt{\frac{KT}{2\,\rho_{np}R_{np}}}f(T,\phi) \quad (37)$$

where, Boltzman Constant: $k = 1.3807\times 10^{-23} J/K$

$$f(T,\phi) = (2.8217\times 10^{-2}\phi + 3.917\times 10^{-3})\left(\frac{T}{T_0}\right) + (-3.0669\times 10^{-2}\phi - 3.391123\times 10^{-3} \quad (38)$$

For 1% ≤ ϕ ≤ 4% and 300K<T>325K

The effective viscosity can be obtained using following mean empirical correlations:

$$\mu_{eff} = \mu_f \times \frac{1}{(1-34.87\,(d_p/d_f)^{-0.3}\times \emptyset^{1.03})} \quad (39)$$

$$d_f = \left[\frac{6M}{N\pi\rho_{fo}}\right]^{\frac{1}{3}} \quad (40)$$

where:
M: is the molecular weight of base fluid.
N: is the Avogadro number = 6.022×10^{23} mol^{-1}.
ρ_{f0}: is the mass density of the based fluid calculated at temperature T_0=293K.

2.2 Numerical Solutions

The numerical methodology is based on finite volume method. Computer fluid dynamic (CFD) code which is FLUENT solver was used. The computational mesh was generated by using Gambit software, then the numerical model, initial boundary conditions, assumptions, and other numerical values are defined. The value which is lower than 10^{-6} was used for the convergence criterion of Fluent iteration process.

The three-dimensional channel used in the simulations are square channel. The channel dimension is assumed to be $0.02\times0.02\times1.6\ m^3$ and the other characteristics of the geometry are collected in Table 1. Figure 2 shows the schematic diagram of the problem. Consider a straight duct of uniform rectangular cross section. Let *x* denote the axial direction while *y* and *z* denote the

coordinates of the cross section. The velocities corresponding to these coordinate directions are *u*, *v* and *w* respectively.

Table 1
Geometrical parameters

Parameters	Range
Hydraulic Diameter of Duct (D_h)	0.02m
Channel height, (*h*)	0.02m
Channel width, (*W*)	0.02m
Channel length (*L*)	1.6m

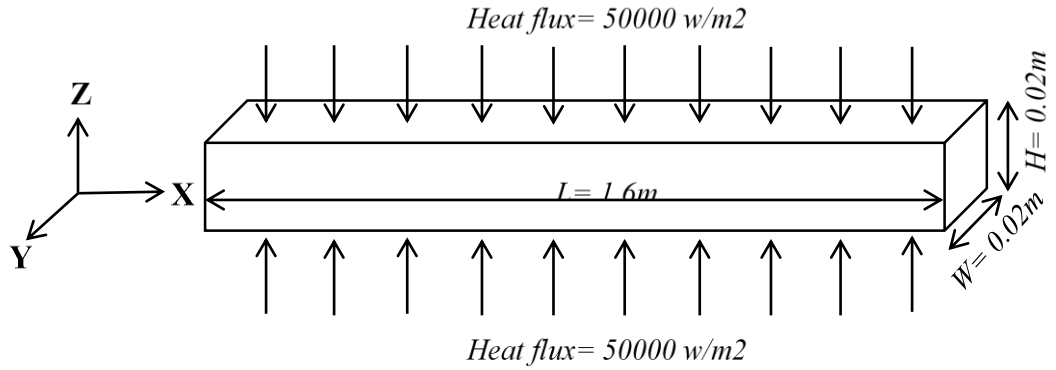

Fig. 2. Geometry parameters

The thermophysical properties of base fluid (water) is listed in Table 2. Table 3 listed the effective thermophysical properties of Al_2O_3-Water and $TiO2$ -Water, ϕ in the range of 1%-3% and d_p of 20nm. Whereas, the effective thermophysical properties of CuO-Water, ϕ in the range of 1%-4% and d_p of 20nm is listed in Table 4.

Table 2
Thermophysical properties of base fluid (water) at T=293 K^o

Thermophysical properties	Water
Density, ρ ($\frac{Kg}{m^3}$)	99.7
Specific heat, C_p($\frac{J}{Kg.K}$)	4178.9
Thermal conductivity, k ($\frac{W}{m.K}$)	0.6
Dynamic viscosity, μ ($\frac{Ns}{m^2}$)	0.000949

Table 3
Effective thermophysical properties of Al_2O_3-Water and $TiO2$ -Water, ϕ in the range of 1%-3% and d_p of 20nm

Thermophysical properties	d_p =20nm	
	Al_2O_3	TiO_2

	ϕ= 1%	ϕ= 2%	ϕ= 3%	ϕ= 1%	ϕ= 2%	ϕ= 3%
$\rho\ (kg/m^3)$	1027.4	1057.2	1086.9	1030.2	1062.8	1095.3
$C_p(J/kg.K)$	4046.96	3922.46	3804.78	4034.79	3899.52	3772.3
k (W/ $m.K$)	0.617	0.635	0.653	0.615	0.63	0.6464
$\mu\ (Ns/m^2)$	0.00102	0.00113	0.00126	0.00132	0.00154	0.0018

Table 4
Effective thermophysical properties of CuO-Water, ϕ in the range of 1%-4% and d_p of 20nm

Thermophysical properties	d_p =20nm			
	Al_2O_3			
	ϕ= 1%	ϕ= 2%	ϕ= 3%	ϕ= 4%
$\rho\ (kg/m^3)$	1027.4	1057.2	1086.9	1210.2
$C_p(J/kg.K)$	4046.96	3922.46	3804.78	3418.5
k (W/ $m.K$)	0.617	0.635	0.653	0.665
$\mu\ (Ns/m^2)$	0.00102	0.00113	0.00126	0.00304

3. Results

3.1 Preliminary Results

3.1.1 Validation of Reynolds number

The three-dimensional channel simulations were performed to analyse the local Nusselt number for specific Reynold numbers, average Nusselt number in a range of Reynolds number for square straight channel and friction factor in a range of Reynolds number. A careful check for the grid-independence of the numerical solution has been made to ensure the accuracy and validity of the numerical scheme. For this study, grid system are 151× 41×41, 181×61×61 and 151 × 61×61 have been tested and the results of these cases were compared with the previous work. So, in view of saving computation time, a grid system of 151 × 61×61 (151 nodes in the length and 61 nodes in the height and width directions) were adopted in the computations.

The secondary flow configuration for the case of local Nusselt number for specific Reynold numbers are plotted in Figure 3. Figure 3(a) is the result obtained from this study and Figure 3(b) is the result obtained from the Raiesi *et al.,* [33]. This is the results of the Reynold numbers, Re= 2236. As can be seen from figure, the coarse and fine meshes results obtained from the simulation (Figure 3(a) has a good agreement with the result obtained from previous work [33] (see Figure 3(b)).

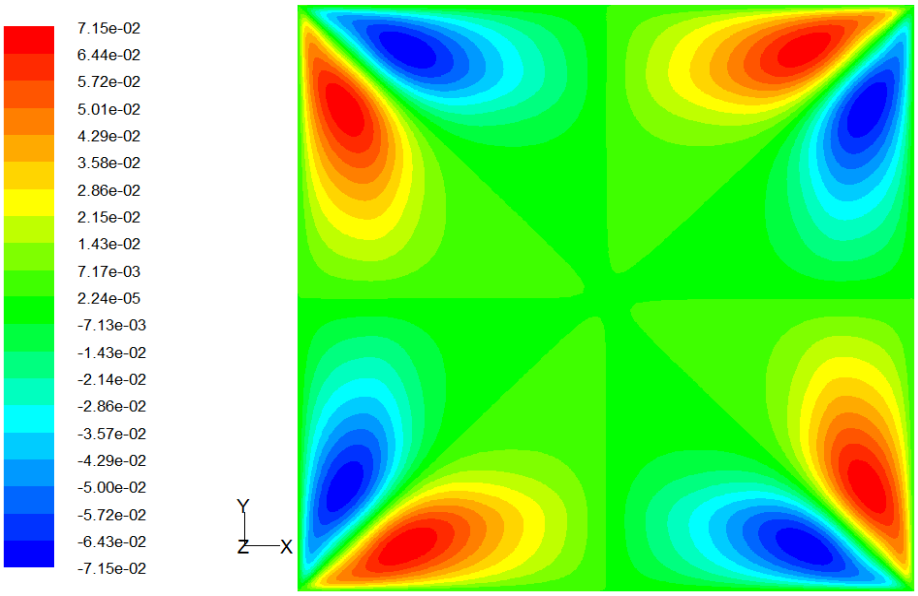

(a)

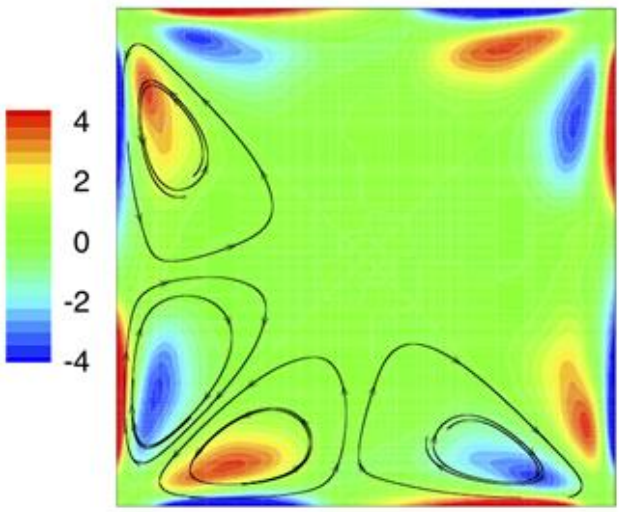

(b)

Fig. 3. Validation the computational code with Reynolds number, Re = 2236 (a) simulation result using CFD code, (b) simulation result from previous work [33]

3.1.2 Validation of friction factor

Important physical aspect of these flows is the presence of secondary motions in the plane perpendicular to the streamwise direction. The secondary motion of the turbulent flow through a straight duct is driven purely by turbulent stresses. Although the velocity of this secondary motion is only of the order of 2-3% of the bulk streamwise velocity, its very presence has far-reaching consequences, it causes bulging of the velocity contours towards the channel corner, hence affecting sediment transport and heat transfer characteristics in the flow.

In order to demonstrate the validity and precision of the model as well as numerical procedure, the friction factor was calculated (Eq. 26) and compared with the Darcy friction correlation given by Blasius which is presented from Eq. (32). Figure 3 shows the results of the friction factor calculated from Eq. (26) and from Blasius formula in Eq. (32). As it is shown in Figure 4, good agreement between

the computed predictions and the theoretical results are observed over the range of the Reynolds number studied. Figure 5 shows the comparison of the friction factor obtained from pure water and CuO, Al_2O_3 and TiO_2. As can be seen from Figure 5, the friction factor is constant in all cases, although calculated with different types of nanofluid (CuO, Al_2O_3 and TiO_2). It can be seen that different types of nanofluids do not influence the friction factor values.

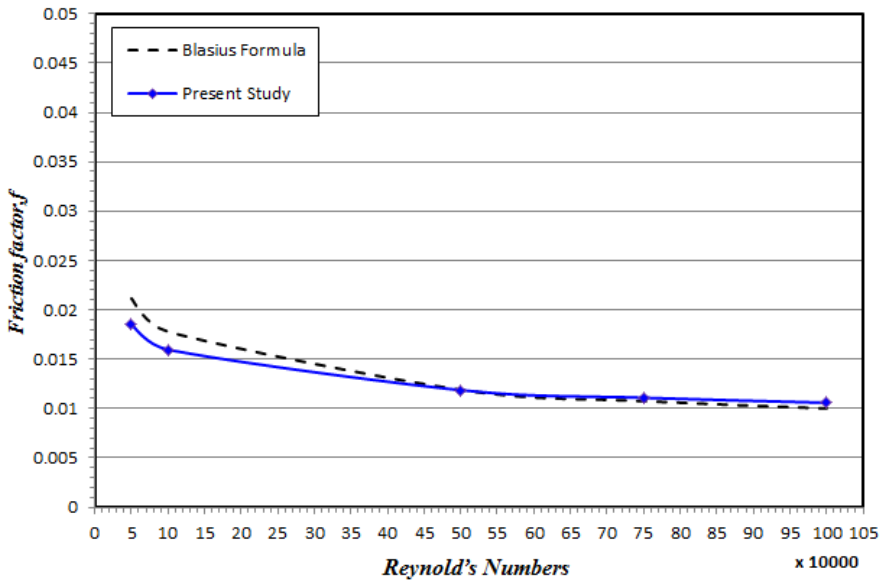

Fig. 4. Comparison of the Darcy friction factor and the Blasius formula against thecomputed values for water in turbulent regime

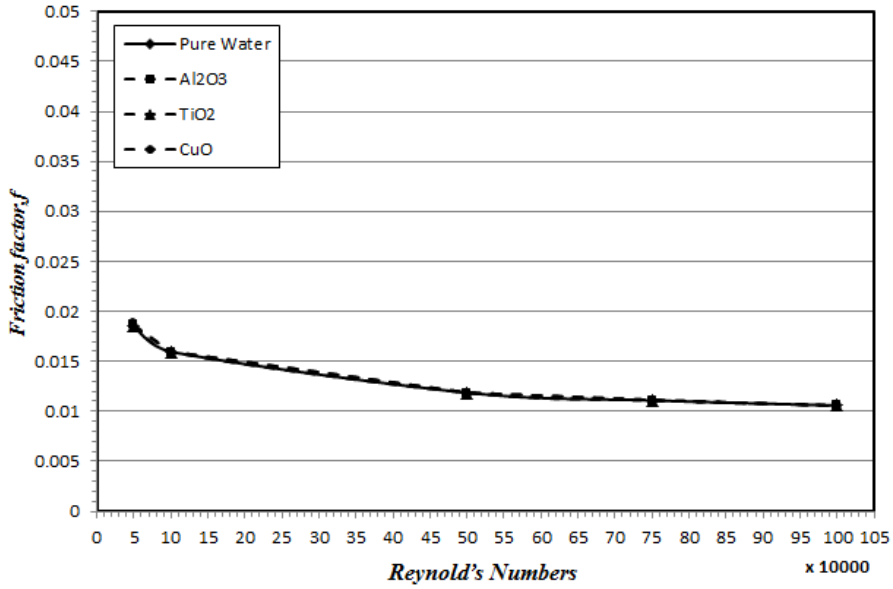

Fig. 5. Comparison of the computed values for pure water and nanofluids in turbulent regime

4. Conclusions

The present study was conducted to evaluate the fully developed turbulent flow on secondary flow configuration, heat transfer, friction factor, flow characteristics and nanofluids parameters through square straight channel. The three-dimensional channel simulations were performed to

analyse the local Nusselt number for specific Reynold numbers, average Nusselt number in a range of Reynolds number for square straight channel and friction factor in a range of Reynolds number. The preliminary results show that the results from the simulation have a good agreement with the previous work. Based on this study, the following recommendations could be made for the future work.

i. The heat transfer and fluid flow characteristics of fully developed square straight channel could be investigated experimentally in order to compare the numerical results having obtained from the current study.
ii. This study can be extended to other types of working fluids or base fluids with the same or new type of nanoparticles.
iii. The geometry of this study can be investigated with various boundary conditions.
iv. Investigating the usage of two-phase model in the numerical analysis.
v. Investigating of the unsteady flow in the current geometry.

A numerical study of three-dimensional of thermal and turbulent fluid flow through skewed channel can be done.

Acknowledgement
Authors would like to acknowledge Takasago Thermal Engineering Ltd and Universiti Teknologi Malaysia (Grant no. 4B314) for supporting this research activity.

References

[1] Schlichting, H., J. Kestin, and Robert L. Street. "Boundary-Layer Theory." (1980): 125-125.
[2] Bradshaw, Peter. "Turbulent secondary flows." *Annual review of fluid mechanics* 19, no. 1 (1987): 53-74.
[3] Joung, Younghoon, Sung-Uk Choi, and Jung-Il Choi. "Direct numerical simulation of turbulent flow in a square duct: analysis of secondary flows." *Journal of engineering mechanics* 133, no. 2 (2007): 213-221.
[4] Haque, M. A., A. K. A. Hassan, J. T. Turner, and H. Barrow. "An observation on the origin of secondary flow in straight noncircular ducts." *Wärme-und Stoffübertragung* 17, no. 2 (1983): 93-95.
[5] Thangam, Siva, and C. G. Speziale. "Non-Newtonian secondary flows in ducts of rectangular cross-section." *Acta mechanica* 68, no. 3-4 (1987): 121-138.
[6] Longatte, Florent, François Avellan, and Jean-Louis Kueny. "Three-dimensional analysis of the flow in the Ercoftac draft tube with N3S and fluent softwares." In *Workshop Ercoftac 99*, no. CONF, pp. 20-23. 1999.
[7] Gyr, Albert, and Johannes Bühler. "Secondary flows in turbulent surfactant solutions at maximum drag reduction." *Journal of Non-Newtonian Fluid Mechanics* 165, no. 11-12 (2010): 672-675.
[8] Uhlmann, Markus, Alfredo Pinelli, Genta Kawahara, and Atsushi Sekimoto. "Marginally turbulent flow in a square duct." *Journal of fluid mechanics* 588 (2007): 153-162.
[9] Pinelli, Alfredo, Markus Uhlmann, Atsushi Sekimoto, and Genta Kawahara. "Reynolds number dependence of mean flow structure in square duct turbulence." *Journal of fluid mechanics* 644 (2010): 107-122.
[10] Pattison, Martin J., Kannan N. Premnath, and Sanjoy Banerjee. "Turbulence-Induced Secondary Flows in a Square Duct using a Multiple-Relaxation-Time Lattice-Boltzmann Approach." In *TSFP DIGITAL LIBRARY ONLINE*. Begel House Inc., 2007.
[11] Zhu, Zuojin, Hongxing Yang, and Tingyao Chen. "Numerical study of turbulent heat and fluid flow in a straight square duct at higher Reynolds numbers." *International journal of heat and mass transfer* 53, no. 1-3 (2010): 356-364.
[12] Lai, W. Y., B. Duculescu, P. E. Phelan, and R. S. Prasher. "Convective heat transfer with nanofluids in a single 1.02-mm tube." In *ASME 2006 International Mechanical Engineering Congress and Exposition*, pp. 337-342. American Society of Mechanical Engineers Digital Collection, 2006.
[13] Xuan, Yimin, and Qiang Li. "Investigation on convective heat transfer and flow features of nanofluids." *J. Heat transfer* 125, no. 1 (2003): 151-155.
[14] Choi, Stephen US, and Jeffrey A. Eastman. *Enhancing thermal conductivity of fluids with nanoparticles*. No. ANL/MSD/CP-84938; CONF-951135-29. Argonne National Lab., IL (United States), 1995.
[15] Clark, M. James. *Electricity and magnetism*. Clarendon Press, Oxford, 1873.
[16] Qingzhong, X. "Effective-medium theory for two-phase random composites with an interfacial shell." *Cailiao Kexue Yu Jishu(Journal of Materials Science & Technology)(China)(USA)* 16 (2000): 367-369.

[17] Lee, S., SU-S. Choi, S, and Li, and J. A. Eastman. "Measuring thermal conductivity of fluids containing oxide nanoparticles." (1999): 280-289.
[18] Das, Sarit Kumar, Nandy Putra, Peter Thiesen, and Wilfried Roetzel. "Temperature dependence of thermal conductivity enhancement for nanofluids." *J. Heat Transfer* 125, no. 4 (2003): 567-574.
[19] Wang, Xinwei, Xianfan Xu, and Stephen US Choi. "Thermal conductivity of nanoparticle-fluid mixture." *Journal of thermophysics and heat transfer* 13, no. 4 (1999): 474-480.
[20] Xie, Huaqing, Jinchang Wang, Tonggeng Xi, Yan Liu, Fei Ai, and Qingren Wu. "Thermal conductivity enhancement of suspensions containing nanosized alumina particles." *Journal of applied physics* 91, no. 7 (2002): 4568-4572.
[21] Xuan, Yimin, and Qiang Li. "Investigation on convective heat transfer and flow features of nanofluids." *J. Heat transfer* 125, no. 1 (2003): 151-155.
[22] Putra, Nandy, Wilfried Roetzel, and Sarit K. Das. "Natural convection of nano-fluids." *Heat and mass transfer* 39, no. 8-9 (2003): 775-784.
[23] Chon, Chan Hee, Kenneth D. Kihm, Shin Pyo Lee, and Stephen US Choi. "Empirical correlation finding the role of temperature and particle size for nanofluid (Al 2 O 3) thermal conductivity enhancement." *Applied Physics Letters* 87, no. 15 (2005): 153107.
[24] Godson, Lazarus, B. Raja, D. Mohan Lal, and S. Wongwises. "Enhancement of heat transfer using nanofluids—an overview." *Renewable and sustainable energy reviews* 14, no. 2 (2010): 629-641.
[25] Rostamani, M., S. F. Hosseinizadeh, M. Gorji, and J. M. Khodadadi. "Numerical study of turbulent forced convection flow of nanofluids in a long horizontal duct considering variable properties." *International Communications in Heat and Mass Transfer* 37, no. 10 (2010): 1426-1431.
[26] Guide, FLUENT User'S. "Version 6.2. 16, Fluent Inc." (2005).
[27] Incropera, Frank P., Adrienne S. Lavine, Theodore L. Bergman, and David P. DeWitt. *Fundamentals of heat and mass transfer*. Wiley, 2007.
[28] Eiamsa-ard, Smith, and Pongjet Promvonge. "Numerical study on heat transfer of turbulent channel flow over periodic grooves." *International Communications in Heat and Mass Transfer* 35, no. 7 (2008): 844-852.
[29] Pak, Bock Choon, and Young I. Cho. "Hydrodynamic and heat transfer study of dispersed fluids with submicron metallic oxide particles." *Experimental Heat Transfer an International Journal* 11, no. 2 (1998): 151-170.
[30] Bejan, Adrian. *Convection heat transfer*. John wiley & sons, 2013.
[31] White, F. M. "Viscous Fluid Flow 2nd edition McGraw-Hill." *New York* (1991).
[32] Buongiorno, Jacopo. "Convective transport in nanofluids." *J. Heat Transfer* 128, no.3 (2006): 240-250.
[33] Raiesi, Hassan, Andrew Pollard, and Ugo Piomelli. "Direct numerical simulations of turbulence induced secondary motion in square and skewed ducts." In *TSFP DIGITAL LIBRARY ONLINE*. Begel House Inc., 2011.